Genetic variation and associations involving Fusarium head blight and deoxynivalenol accumulation in cultivated oat (Avena sativa L.)

Journal:	*Plant Breeding*
Manuscript ID	PLBR-15-OA-437.R5
Manuscript Type:	Original Article
Date Submitted by the Author:	n/a
Complete List of Authors:	Bjørnstad, Åsmund; Norges miljo- og biovitenskapelige universitet Institutt for plantevitenskap, He, Xinyao; Norges miljo- og biovitenskapelige universitet Institutt for plantevitenskap, Plant Science; Centro Internacional de Mejoramiento de Maiz y Trigo Gobena, Selamawit; Norges miljo- og biovitenskapelige universitet Institutt for plantevitenskap Klos, Kathy; USDA-ARS Small Grains and Potato Germplasm Research Unit Huang, Yung-Fen ; Agriculture and Agri-Food Canada; National Yang-Ming University, Taipei Tinker, Nicholas; Agriculture and Agri-Food Canada, Eastern Cereal and Oilseed Research Centre Dong, Yanhong ; University of Minnesota Twin Cities Skinnes, Hlege; Norwegian University of Life Sciences, Plant and Environment
Keywords:	Fusarium., Oat, Mycotoxins

Genetic variation and associations involving Fusarium head blight and deoxynivalenol accumulation in cultivated oat (*Avena sativa* L.)

Åsmund Bjørnstad[1*], Xinyao He[1], Selamawit Tekle[1], Kathy Klos[2], Yung-Fen Huang[3], Nicholas A. Tinker[3], Yanhong Dong[4], Helge Skinnes[1]

[1]Department of Plant Science, Norwegian University of Life Sciences, N1432 Ås, Norway

[2]Small Grains and Potato Germplasm Research, USDA-ARS, Aberdeen, ID, U.S.A.

[3]Agriculture and Agri-Food Canada, Ottawa, Canada. (Y-F Huang's current address: School of Life Sciences, National Yang-Ming University, Taipei, Taiwan)

[4]Department of Plant Pathology, University of Minnesota, St. Paul, MN 55108, USA

[*]Corresponding author, e-mail asmund.bjornstad@nmbu.no

Abbreviations: DON = deoxynivalenol; DTF = Days to flowering; DTM= Days to yellow maturity; FHB= Fusarium Head Blight; FS= floret sterility; GWAS = Genome-Wide Association Study; LDA= Linear Discriminant Analysis; PCA = Principal Component Analysis; PH= Plant Height; PLSR= Partial Least Squares Regression; GGE biplot = Genotype by Genotype x Environment Biplot.

Abstract

Resistance in oats (*Avena sativa* L.) to *Fusarium graminearum* was phenotyped in 424 spring oat lines from North America and Scandinavia and genotyped with 2974 SNP markers. Fusarium Head Blight (FHB), deoxynivalenol (DON) content, days to flowering (DTF) and days to yellow maturity (DTM) were scored in field trials in 2011-12. Trials with phenotypic ranges from 1-30 ppm and sufficient accuracy were obtained by an augmented design and spawn inoculation. Discriminant Analysis-PCA identified the different gene pools, with overlaps corresponding to known pedigrees and germplasm exchanges. Structure was negligible and GWAS (Genome Wide Association Study) ~~was~~ done using mixed linear models in TASSEL or Partial Least Squares Regression (PLSR). PLSR ~~allowed~~ allows simultaneous analyses of several phenotypes (~~years,~~ environments and/or ~~traits), especially useful for correlated~~ traits) and ~~,~~is a promising tool for GWAS in plants and should be tested in species with sequenced genomes. FHB was associated with phenology QTLs, due to very susceptible early lines from the Midwest. ~~FHB and DON were moderately correlated and FHB variance was limited in adapted genotypes.~~ Lines with consistently low DON (and early heading) were identified. Six QTLs for DON were not associated with earliness, including three QTLs reported previously.

Key Message: A GWAS of resistance to *Fusarium* (FHB) and the mycotoxin DON in oat is analyzed by TASSEL and PLSR. The latter detected more QTLs, many associated with late maturity.

Contributions by authors:

ÅB: leading and analyzing the field experiments, PLSR analysis and writing the ms; XH: Field notes, analyses in SAS and drafting this part and comparative mapping; ST: Field notes and participating in writing; KK: Performing and writing TASSEL analysis, linkage group analysis; Y-FH: Editing Illumina and GBS data; NAT: Leading the marker work and consensus mapping; YD: Doing all DON analyses; HS: financing, leading and analyzing the field experiments in 2011

Conflict of Interest: The authors declare no conflict of interest.

Formatted: Not Highlight

Formatted: Not Highlight

Formatted: Not Highlight

Formatted: Not Highlight

Formatted: Not Highlight

Introduction

Oat (*Avena sativa* L.) is an important cereal crop, especially in the northern hemisphere, with Russia, Canada and the Nordic countries (Finland, Sweden and Norway) being the largest producers (Marshall et al. 2013). Fusarium head blight (FHB) caused by *Fusarium* spp. has recently emerged as a major biotic constraint to oat production in these regions. In addition to yield reduction, FHB leads to the accumulation of mycotoxins that are toxic to both humans and animals. Deoxynivalenol (DON) produced by *F. graminearum* and *F. culmorum* is the most prevalent *Fusarium* mycotoxin. In the past 15 years, *F. graminearum* has become the major FHB pathogen in the Nordic countries, possibly due to a series of warm and wet years. Since *F. graminearum* produces wind-borne ascospores, while *F. culmorum* does not, *F. graminearum* may be better adapted to cause epidemics. Legislative limits for DON in unprocessed oat and oat-based foods have been set by the European Union at 1,750 and 750µg/kg, respectively (European Commission 2006), reinforcing the importance of FHB and DON control in oat. In Norway, these limits are now enforced through price penalties on every oat crop that exceeds them.

The most susceptible stage of oat for *Fusarium* infection is anthesis, although late infections (or secondary proliferation) may occur up to yellow maturity under wet field conditions (Tekle et al. 2012; Tekle et al. 2013). During anthesis, the fungus enters the floret cavity through the floret apex, colonizing first the anthers and then establishing an infection on the inner surfaces of the palea, lemma, and caryopsis. The disease may spread to adjacent florets within a spikelet, but rarely through the pedicels to neighboring spikelets (Tekle et al. 2012). Early infection usually leads to floret sterility or severely reduced seed germination, as well as to high DON content in the caryopsis, whereas late infection mainly leads to reduced germination and DON accumulation in the hulls (Tekle et al. 2013). Late infection usually occurs in the field without visual symptoms, yet can lead to considerable levels of DON and *Fusarium* damaged kernels (He et al. 2013; Tekauz et al. 2004) .

Oat is generally considered more resistant to FHB than wheat and barley, with less visible FHB symptoms in the field (Langevin et al. 2004; Tekauz et al. 2004). This is due to the wide spacing of the spikelets in the oat panicle (compared to the compact spike structure of wheat and barley)

which minimizes the spread of infection among adjacent spikelets (Bjørnstad and Skinnes 2008; Tekle et al. 2012). For this reason, point inoculation is not suitable for oat (Langevin et al. 2004) while spray and especially spawn inoculation methods have provided reliable results in Norway(He et al. 2013) .

Phenological traits including plant height (PH), days to flowering (DTF), and days to yellow maturity (DTM) often show negative correlations with FHB severity in wheat and barley, where late and tall lines tend to have less disease (Buerstmayr et al. 2009; Emrich et al. 2008; Steffenson et al. 2003). This is partly an artifact, which may be reduced by scoring disease in each line according to phenological stage. In oat, it is more complex. FHB symptoms may often be confounded with maturation of glumes (He et al. 2013). Not surprisingly, the reported effects of phenology on FHB symptoms are unclear. The disease was more severe for late lines in Finland and Russia (Gavrilova et al. 2008; Parikka et al. 2008); whereas early lines were more susceptible in Norway . In terms of PH, Langseth et al. (1995) suggested that tall lines were more resistant, but Gavrilova et al. (2008) did not find a significant correlation. In Norway, the correlations between PH and FHB was significant in one of two mapping populations(He et al. 2013) , where shorter plants showed a moderate association with higher FHB severity.

Genetic mechanisms underlying oat FHB resistance are largely unknown. This may be due in part to the complexity of the oat genome (Oliver et al. 2013; Tinker et al. 2009), the limited availability of cytological and molecular tools (Oliver et al. 2010; Rines et al. 2006), and an under-appreciation of the disease in oat (Campbell et al. 2000). Diversity Array Technology (DArT), the first high-throughput marker type to be used in oat (Tinker et al. 2009), facilitated a series of genetic studies, including the first QTL analysis of resistance to DON accumulation carried out in two mapping populations . As in wheat and barley, resistance to FHB and DON accumulation in oat showed quantitative inheritance, with a few major QTL and numerous minor QTL whose expression was significantly influenced by environment(He et al. 2013) . A QTL for DON content was detected consistently on chromosome 17A/7C in both populations, with phenotypic effects of 12.2–26.6%(He et al. 2013). This chromosome contains a translocation between two sub-genomes within most spring oat varieties, in contrast to the non-translocated versions of 17A and 7C found primarily in winter oats (Jellen and Beard, 2000).

While bi-parental populations provide good localization and characterization of specific gene differences, they do not provide information on the importance and frequency of resistance genes in a generalized population or germplasm base. For this, association mapping (AM) and genome-wide association studies (GWAS) may be helpful (Zhu et al. 2008). The advent of DArT markers and an improved linkage map (Tinker et al., 2009) made GWAS possible for oat, and enabled the first genome-wide studies of linkage disequilibrium (LD) to evaluate and interpret the effectiveness of GWAS (Newell et al. 2010). It was shown that LD in oat extended over shorter distances compared to barley, was relatively consistent across most germplasm clusters, and was mostly free of major population structure other than distinction between spring and winter types (Newell et al. 2010). Subsequently, GWAS was successfully used to identify marker associations with beta-glucan concentration in globally collected oat (Newell et al. 2012) as well as within elite North American oat varieties (Asoro et al. 2013). GWAS of FHB resistance has been reported in wheat (Kollers et al. 2013) and barley (Massman et al. 2011), but not in oat.

Large numbers of single-nucleotide polymorphism (SNP) markers have now become available for oat (Oliver et al. 2011).The first physically anchored consensus map that resolved the 21 oat chromosomes was based on 985 robust SNPs and 68 previously published markers (Oliver et al. 2013). In recent studies this SNP marker platform has been expanded to utilize a 6k Illumina chip (Tinker et al. 2014), and these markers have been supplemented using a genotyping-by-sequencing (GBS) platform (Huang et al. 2014). Combining these resources, two foundation studies were developed: a consensus map based on the larger set of markers mapped in 12 populations (Chaffin et al. 2016), and a study of diversity and population structure, including a GWAS analysis of heading date in 635 oat lines (Esvelt Klos et al. 2016). Since this prior analysis confirmed that the primary population structure present in oat is related to spring vs. winter habit, the current work is focused on a set of spring oat varieties that are a subset of the 635 oat lines used in the aforementioned work. However, within this germplasm, we sought to reassess structure and its effect on GWAS. Software packages that assess population structure (such as STRUCTURE (Pritchard et al. 2000)) try to identify sub-populations that are in Hardy-Weinberg equilibrium, a highly unrealistic goal in an inbreeder like oat. Assumption-free ways to identify groupings are principal component analysis (PCA) (Price et al. 2010) and linear discriminant analysis based on PCA (LDA-PCA) (Jombart et al. 2010). While PCA itself has been frequently used, the latter has been less tested in plants.

PCA has also been successfully used in QTL analysis in bi-parental populations through the GGE biplot approach (Yan and Tinker 2005; Yan et al. 2005). In a biplot, closely linked markers will cluster and so will associated QTLs. The authors suggested that "the association of a marker with the trait is approximated by the length of the marker vector multiplied by the length of the environment vector multiplied by the cosine of the angle between the two vectors" (p.321).

PCA decomposes and models the data into orthogonal linear components of decreasing importance, and a PCA biplot presents (usually) the main axes of variance in either the markers (the X matrix) and the traits (the Y matrix) in a bi-linear way. A further development is Partial Least Squares Regression (PLSR) which models the covariance of X and Y. This algorithm was developed in spectroscopy (chemometrics) to handle data sets where the number of variables (wavelengths) far exceeds the number of samples and where the variables have strong collinearities (Martens and Naes 1992). This is also the case in current genomic data sets with typically tens of thousands of marker genotypes and phenotypes from at best a few hundred individuals. PLSR has been less used to analyze marker-phenotype relationships. Boulesteix and Strimmer (2007) found it a "versatile tool" in gene expression studies, incl. classification. In a study of obesity traits in humans, Xue et al. (2012) found by simulation that PLSR had greater power and more efficiently related causal SNPs to correlated traits underlying a "latent" phenotype. Using "sliding windows" of up to 12 SNPs was more efficient than linear regression of one trait and marker at a time. Recently, Dumancas et al (2015) compared the common chemometrical dimension-reducing methods like Principal Component Regression (PCR) and PLSR in GWAS, to the usual single marker-single phenotype or multiple linear regression. From their perspective,genetical epidemiology, both cases and theory recommended more use of PCR and PLSR. To our knowledge PLSR has not been used for GWAS in plants, but for linkage and QTL analysis in bi-parental populations (Bjørnstad et al. 2004).

Both PCA and PLSR represent exploratory "soft" modelling approaches, as distinguished from traditional "hard" modelling based on assumptions about distributions etc. to allow significance testing and choice between models. Typical "soft" models are visual, it is recommended to "plot a lot", using score plots of samples, loading plots (variables), biplots or regression plots, stability plots of cross validation deviations etc., besides in-built methods to

Formatted: Not Highlight
Formatted: Not Highlight
Formatted: Not Highlight
Formatted: Not Highlight
Formatted: Not Highlight
Field Code Changed
Formatted: Not Highlight
Formatted: Not Highlight
Formatted: Not Highlight
Formatted: Not Highlight
Formatted: Not Highlight
Formatted: Not Highlight

identify outliers in samples or variables. In data with high numbers of variable tests, "hard" models will usually demand higher pre-set significance levels, whereas "soft" models will try to identify spuriously significant variables by techniques like cross-validation. Both "hard" and "soft" methods may be used in the same study, like in our case.

The objectives of this study were (1) to evaluate FHB severity, DON level and floret sterility (FS) in a population of spring oat germplasm; (2) to assess the relationship between FHB resistance and PH, DTF and DTM; (3) to evaluate genetic diversity and population structure using alternative assumption-free methods such as PCA and LDA-PCA; and (4) to identify QTLs for FHB resistance using GWAS by a mixed linear model (MLM) and compare this to results using PLSR.

Materials and methods

Plant materials

A set of 424 oat lines originating primarily from 11 spring oat breeding programs (Table S1) were used in this study. These included: 267 lines nominated from six breeding programs in USA; Purdue University(PURD); University of Illinois (ILL); University of Minnesota (MINN); University of Wisconsin (WISC); USDA-ARS in Aberdeen, Idaho (ABER); North Dakota State University (NDSU), plus one check, Horizon270, from Louisiana State University (LSU); 131 lines from three breeding programs in Canada (AAFC, Winnipeg/Brandon, Manitoba, (WNPG); CDC, University of Saskatchewan (SASK); AAFC Ottawa, Ontario (OTTW)); and 26 lines from Nordic breeding programs (Norway, NRWY with Sweden and Finland pooled as NORD).

Field experiments

The plant materials were tested using an un-replicated augmented design with replicated checks in 2011 and 2012 at the Vollebekk research farm, Norwegian University of Life Sciences, Ås, Norway. The experiment had 12 rows, 40 columns, and eight blocks, each containing the same set of two moderately resistant (Hurdal and Leggett) and four susceptible checks (Bessin, Gem, Ogle, and Horizon270). This gave eight independent values for each of the six checks. Plots were

0.45 x 2.0m spaced 0.3m apart and the alleys between blocks were 1m wide. Each plot was sown with 50g of seeds in four rows spaced 0.15m apart. A compound fertilizer (NPK 21-4-10) was applied just before planting at a rate of 400kg/ha. Plants were spawn inoculated with *F. graminearum* infected oat kernels at Zadoks 31/32 stage (Zadoks et al. 1974). The spawn inoculum was prepared following the procedure described by Skinnes et al. (2010) and distributed evenly at a rate of 10g/m^2 during the stem elongation stage (32/33). Following spawn inoculation, the field was mist-irrigated for 5 minutes at 15 min intervals from 19.00 h to 22.00 h, as described by He et al. (2013).

Phenotyping

Phenological traits. DTF was recorded when approximately 50% of the panicles in a plot had fully emerged. DTM was recorded when half of the panicles were at yellow maturity. PH was measured at maturity, from the ground to the panicle top of average plants.

Fusarium traits. In 2011, FHB was scored twice, with a one-week interval, using a zero to four scale, with zero equivalent to no apparent FHB symptom in the plot and four for> 80% symptomatic spikelets. In 2012, FHB was scored three times, at three- and four-days intervals, using a zero to five scale. In order to make the FHB scores in the two years comparable, the 2011 data were amplified 1.25 times to transform the scale from zero to four to zero to five. The area under the disease progress curve (AUDPC) was calculated from the disease evaluations and used in all subsequent analysis as FHB severity. Data on FHB in each year and their mean are abbreviated as FHB11, FHB12 and FHB_M, and similarly in all traits.

Care was taken during harvesting not to lose shriveled grains, and seeds were threshed carefully indoors to minimize this. Still some loss was unavoidable, especially in highly susceptible genotypes. To possibly correct this, 15 randomly sampled panicles were sampled from each plot in 2012, and floret sterility (FS (%)) was calculated as the number of empty spikelets divided by the total number of spikelets. In both years, 70g of kernels from each plot were sent to the University of Minnesota for DON analyses. DON level was determined from a four gram ground subsample using the GC/MS method as described by Mirocha et al. (1998) and Fuentes et al. (2005). Weighted DON in 2012 was estimated as wDON = DON/(1-FS).

Genotyping

Genotyping was performed as reported in a co-submitted work using an iSelect 6K bead chip array (Illumina, San Diego, USA) and genotype-by-sequencing (GBS). Genotypes for 4,975 EST-derived SNPs were acquired at the USDA-ARS Genotyping Laboratory at Fargo, ND, as described by Tinker et al. (2014). SNP genotype calls were made with Genome Studio v2011.1 (Illumina, San Diego, USA) with Gen Call set at 0.15. Genotypes for additional SNPs were acquired through GBS using methods described by Huang et al. (2014). SNP genotype calls were made from sequenced *Pstl-Mspl* complexity reductions using the UNEAK pipeline (Fu et al., 2012) with $3x10^8$ as the maximum reads per sequence, $9 x10^8$ as the maximum merged tag count, merging of multiple samples per line, and maximum error tolerance rate of 0.02. Final population filtering of SNPs from both platforms was applied with a call rate ≥0.95, MAF ≥0.01, and heterozygosity ≤0.05 for population structure analysis and GWAS.

Analysis of phenotypic data

Analysis of variance (ANOVA) of phenotypic data was carried out with the PROC GLM module in SAS program ver. 9.2 (SAS Institute, Inc., Cary, NC) according to Scott and Milliken (1993), calculating trait values in each year and year means. The variable *X* was set for experimental genotypes, taking the values of entry numbers for experimental genotypes and zero for checks, whereas the variable *C* was set for checks that takes the values of entry numbers for checks and zero for experimental genotypes. C was considered a fixed effect, the rows, columns and X(C) as random in the ANOVA model:

$$Y_{ij} = \mu + b_j + C_i + X_i(C_i) + \sum_{ij}$$

where b_j denotes the block effect, and C_i and $X_i(C_i)$ denotes the entry effect. FHB and DON were also calculated with DTF, DTM, or PH as covariates, in total 34 phenotypic traits. For association analyses, both best linear unbiased prediction (BLUP) and best linear unbiased estimation (BLUE) values were calculated using the *solution* function in the PROC MIXED

Formatted: Not Highlight

Formatted: Not Highlight

module, with X(C) as random or fixed, respectively. Pearson correlation coefficients were calculated between the BLUP and BLUE values, and between traits and BLUPs in the PROC CORR module.

Formatted: Not Highlight

Marker data were binarized by setting the 'AA' scores as '1' and 'BB' scores as '0', while heterozygotes were pooled with missing calls. The 11 breeding programs (SASK, WNPG, OTTW, NDSU, MINN, WISC, PURD, ILL, LSU, NRWY and NORD), or germplasm groups (largely geographical groupings identified by LDA-PCA, see below) were included as categorical variables.

Population structure analysis

Population structure in the marker data was investigated in three different ways.

First, model-based structure analysis was performed, using ADMIXTURE v1.23 (Alexander et al. 2009) under the default settings, to find the optimal value of k ancestral groupings. A subset of 340 unlinked SNPs in linkage disequilibrium was used for the model-based structure analyses.The SNPs were identified in PLINK v1.07 (Purcell et al., 2007; http://pngu.mgh.harvard.edu/purcell/plink/) by removing SNPs within a 20-SNP sliding window (advanced with a step of 5 SNPs) with $r^2 > 0.1$. Models were evaluated by plotting the cross-validation error against the number of sub-populations in the model.

Second, relative genetic diversity within and among populations (breeding programs or germplasm groups) were analysed by AMOVA using GenAlEx ver. 6.4 (Peakall and Smouse 2006) and F_{ST}-values (Nei 1973) were calculated.

Third, LDA-PCA was performed with the 11 breeding programs as categorical variables, using the multivariate package of *The Unscrambler* (Version 10.3, CAMO Software AS, Oslo, Norway, www.camo.com). A "confusion matrix", showing actual vs predicted groups, was generated. Based on these results, the breeding programs were grouped based on similarity, and a new confusion matrix generated.

GWAS using PCA and MLM

Genotype-phenotype association was tested using MLM in TASSEL v4 (Bradbury PJ 2007) under the default settings. Population structure was also accounted for by incorporating the first three principal components (PC) as covariates in the model. Cryptic relatedness among lines was accounted for using a kinship matrix. Both the PC and kinship were estimated using all SNPs without missing data. The relationship between genotype and phenotype was also modelled by incorporating DTF or PH as covariates. Results are reported for SNPs present in the homozygous state in at least five lines and with locations on linkage groups and distances based on the revised oat consensus map (co-submitted), where consensus chromosome representations were designated as *Mrg01* to *Mrg33* while putative corresponding physical chromosomes were appended where supported by most recent evidence.

GWAS using PCA and PLSR

Principal component analysis was conducted with *The Unscrambler* using all markers (the X matrix) or phenotypes (the Y matrix). The scores and loadings plots were visualized using the *Sample grouping* option, color-coding the breeding programs or germplasm groups in two or three dimensional plots.

The analytical bases of PCA and PLSR are simply and well explained by Martens and Kohler is bilinear, i.e. it reduces the dimensions in often overwhelming data sets seeking the "latent variables" as the linear combinations of markers that maximize the variance in X and Y. PCA decomposes a **X** (NxK) matrix into a model centre, a series of **A** PCs with scores (**t**) and loadings (**p**) vectors in the new **A** space, and an unexplained error (see the Appendix in Martens and Kohler at https://staticcontent.springer.com/esm/art%3A10.1162%2Fbiot.2009.4.1.29/MediaObjects/13752_2015_4010029_MOESM1_ESM.pdf):

$$\boldsymbol{X} = x^{T}_{0} + t_1 \bullet p^{T}_{1} + t_2 \bullet p^{T}_{2} + \ldots + t_a \bullet p^{T}_{a} + \ldots + t_A \bullet p^{T}_{A} + E_A$$
$$= x\mathbf{T}_0 + \mathbf{T}_A \bullet \mathbf{P}^{T}_{A} + \mathbf{E}_A$$
$$= \hat{\mathbf{X}} + \mathbf{E}_A$$

The latent variables are derived from a weighted sum of the original K variables:

Formatted: Not Highlight

Formatted: Font: Italic, Not Highlight

Formatted: Not Highlight

Formatted: Justified, Line spacing: Multiple 1.15 li

Formatted: Not Highlight

Formatted: Font: (Default) Calibri, 11 pt, Not Superscript/ Subscript, Not Highlight

Formatted: Not Highlight

$t_a = (\mathbf{X} - x'_0)v_a$

The same applies to the Y matrix. As shown by Yan et al., this allows a simultaneous analysis of several traits at the same time and identification of markers associated with them, if there is pleiotropy etc.

The extension to PLSR is mainly by including the covariance between X and Y, which means that the X variables *relevant* to explaining the Y variance are used. Therefore their weights in the model may be different. Formally, "a simultaneous PCA of two data tables, $\mathbf{X} = \mathbf{T}_A \bullet \mathbf{P}^T_A$ and $\mathbf{Y} = \mathbf{T}_A \bullet \mathbf{Q}^T_A$, and a regression method that allows the prediction of Y from X, $\mathbf{Y} = \mathbf{X} \bullet \mathbf{B}_A$ ((Martens and Kohler 2009), p.39). Latent variables will be orthogonal and used in regressing Y on X. Unlike PCA, PLSR is able to model and *predict* trait values from the latent variables and estimate the degree of explained "calibration" variance in X and Y. The first is a "full" model, with all markers included. Then the model is reduced by deleting irrelevant markers. By cross-validation, leaving (one or more) samples out and recalculating the models, the deviation variance from the full model is estimated. This then allows the identification of markers with significant regression coefficients, with confidence intervals not spanning zero. ~~This validation usually.~~ Many markers will no longer be significant in the validated model, which leads to a drop in regression R^2. In a second model including only validated and significant markers, the R^2 will again increase and approach the calibration. This model improvement can be rerun and cross-validated several times to find the optimal dimensionality, when explained variances no longer increase or decline. The final model should only have the latent variables necessary to identify the markers associated with each of them. The phenotypic traits may be analyzed individually (e.g. FHB11, FHB12 or FHB_M) or together, in any combination.

In a score plot, positions of genotypes are displayed, like in PCA. The percentages of explained variance in X and Y are indicated in the percentages on each axis. The genotypes may be colour coded by groupings. In a PCA biplot, marker genotypes with high values (allele 1) located close to high values of a certain Y variable (e.g. disease score) indicate susceptibility. If they are diagonally opposed, allele *1* is associated with low disease scores and resistance, and vice versa for the allele *0*. Similarly, if several Y variables are included in the model, diagonal positions mean strong negative correlations due to linkage or pleiotropy. Especially useful is the

Formatted: Not Highlight

Formatted: Not Highlight

Formatted: Not Highlight

"correlation loadings" biplot, where X and Y loadings are standardized as correlation coefficients spanning from -1 to +1 on each axis. Marker variables with coefficients at +/-0.7 or more on each axis, then will have R^2> 49%. By drawing a circle through these points, the most interesting markers are displayed.

In our data all traits were first regressed singly or together using the whole marker matrix. Results are reported in Table 6. However, to illustrate the multi-trait approach, only the joint analysis of FHB_M, DTF_M, and DTM_M is reported in detail (Fig. 5A-F). First, the full model was tested with full (leave-one-out) cross validation and significant markers identified (Fig 5A). In the score plot (Fig 5B) each genotype was color coded according to their 11 breeding programs. The regression plot (Fig 5C) then displayed the calibration and validation lines in the full model. The significant markers indicating possible QTLs (highlighted by circles in the plots) were then included in an optimized model and rerun times until the degree of explained variance was maximal (least prediction error). Fig. 5D shows the correlation loadings biplot optimized after three runs, with significant markers along PC1 and PC2 indicated, as well as significant markers associated with higher PCs located in the "crowd" (note that many markers are no more significant). The axes show that the percentages of explained variance have improved, as indicated in the better calibration and validation fit in the new regression plot (Fig. 5E). The new score plot (Fig. 5F) indicates that the model has grouped genotypes in a different way.

The whole analysis was repeated for each linkage group (Mrg) where a QTL was indicated. The chromosomal positions of markers were then identified from the map (Chaffin et al. 2016) and considered as putative QTLs. Markers significantly associated with traits were then compared to the consensus map positions and with the results from TASSEL. Unless otherwise specified only the *validated* variances explained by a PLSR model are reported in this paper.

Formatted: Not Highlight

Formatted: Not Highlight

Results

Phenotypic evaluation

BLUPs and BLUEs gave highly correlated and equivalent values (>0.99 for FHB11 and FHB12, 0.97 for DON11 and 0.89 for DON12). ~~The~~ As expected, the ~~ranges in~~ BLUP values were ~~reduced~~ shrunk ~~by 30-50%~~ in relation to BLUEs. E.g., for~~mostly affecting the high values that sometimes~~DON12, the BLUP range was 2.2-33.2 ppm, the BLUE 10.2-66.2, ~~exceeded the observed.~~ This did not affect the ANOVA (see Discussion ~~Given this and the limited replication in the Augmented design (although two balanced data sets from two years help), we preferred BLUP to BLUE due to the variance shrinkage (see also Piepho et al. (2008)~~ on this point).

In 2011, AUDPC values for FHB ranged from 2.4 to 26.8, and DON content varied from 4.6 to 48.6 ppm (Table S1). In 2012, the disease level was higher, reflected in both the phenotype distributions (Fig. 1) and the grand means (Table S1) of FHB and DON. Significant 'line' effects were detected by ANOVA for both FHB and DON, as were the 'year' effects, particularly for DON (Table 1). A moderately high correlation of 0.70 was found for FHB between 2011 and 2012. However, correlations between DON11 and DON12 as well as between FHB and DON in single years were much lower, ranging from 0.37 to 0.39 (Table 2). True DON-values were probably underestimated because highly infected florets tend to shrivel and be discarded together with the chaff during harvesting. This was indicated by the check cv. Horizon270, a very precocious dwarf variety from Louisiana. It was consistently the most affected by FHB in the field, but was not among the highest in DON. All the FHB parameters exhibited significant correlations with FS, but the values were generally low (Table 3). Weighting of FHB scores and DON values by FS only marginally affected the results (Tables 2 and 3).

Correlations of FHB and DON with phenology were all significant (Table 3). All correlations were negative, indicating that late and tall oat lines tended to have less disease. Among the three phenological traits, DTF had the biggest impact on FHB and DON, followed by DTM and PH.

A number of related as well as unrelated sources of resistance deriving from several breeding programs were identified. Figure 2 shows that the checks covered the disease range well. Horizon270 was the most susceptible while Leggett (bred in SASK) was consistently the least diseased, but not significantly different from its progenies with OT2022, nor the cv. Stride (OT2022 x 01RAT23) and a sister line. The cv. Odal, currently the most resistant grown in Norway, came close, as did a few lines from OTTW, MINN, NDSU and ABER. The lines

Formatted: Not Highlight
Formatted: Not Highlight
Formatted: Not Highlight
Formatted: Not Highlight
Formatted: Not Highlight
Formatted: Not Highlight
Formatted: Not Highlight
Formatted: Not Highlight
Formatted: Not Highlight
Formatted: Not Highlight

derived from ILL and IND were the most susceptible, but had also the widest range, whereas lines from other programs were more resistant (Fig. 2). Among lines originating in the Midwestern USA, no clear clusters were found for individual states, but MINN had a higher proportion of resistant lines than IND, while ILL and WIS had similar proportions of resistant and susceptible lines.

Molecular data

After manual SNP annotation within Genome Studio and refining the SNP call further with custom software, 1,932 polymorphic markers with no missing data were retained. After filtering additional SNPs through GBS population the total numbers were 2974 SNPs (1737 from ESTs, 1237 from GBS).

Population structure based on marker data

The final matrix dimensions of phenotypic and genotypic data were 418 lines x 3019 traits, the latter comprising 34 phenotypic BLUPs and 2974 markers. The model-based population structure analysis had no clear optimum number of ancestral populations, but PCA displayed three clear clusters. For this reason, we selected k = 3 for further model-based analysis (Figure 3A, B). PC1 (explaining 8.9% of variation) separated samples from breeding programs in the Midwest USA from Canadian and NDSU, PC 2 (5.5%) identified ABER, and PC3 (4.5%) the Nordic lines. It was also evident that the Nordic lines showed considerably less diversity, reflected by closer coordinates (Fig. ~~3~~S1, A-C).Variances using the 1932 markers (without missing data) were nearly the same, indicating a stable pattern (not shown).

The AMOVA of genetic diversity within and among populations also showed only modest differentiation among breeding programs or germplasm groups. Breeding programs accounted for only 6% of the diversity, while 93% was due to variation among lines. When pooled into germplasm groups (see below), the corresponding figures were 13% and 87%.

For LDA-PCA, the 418 lines x 1966 matrix, comprising 34 phenotypic BLUPs and 1932 markers was used. The "confusion matrix" (Table 4A) predicted, on average, 67% of lines correctly to their respective breeding programs. Those originating from the Midwest USA were most often misclassified ("confused") from their respective Midwestern breeding program. Misclassification

Formatted: Highlight

Formatted: Highlight

was also common for lines with a Canadian/NDSU origin, with NDSU, MINN and OTTW gradually overlapping. The ABER lines were rarely misclassified, confirming their distinctness in the PCA. Depending on distance measure, some Nordic lines were classified as Canadian or Midwestern, or vice versa. Such "inaccuracies" correspond well with known germplasm exchange and pedigrees, as does the grouping of NORD and NRWY. For example the SASK cv. 'Triactor' which was classified as NORD has a Swedish parent, while 'Triple Crown' is a Swedish cultivar released in Canada and used as a parent in SASK, WNPG and NDSU. After amalgamation into four germplasm groups (Table 4B), LDA_PCA had classification accuracy of 87%.

The influence of this structure was assessed by PLSR of the germplasm groups on the marker data. At first numerous (>300) markers were associated with the structure, but model optimization indicated that only a few dozen (often representing clusters) could account for this structure (results not shown). This was reasonable given the results from the model-based structure analyses as well as the AMOVA. The residual matrix, from regressing the germplasm groupings on markers and then on phenotypes (FHB or DON), yielded essentially the same pattern as the original data: the same lines were predicted as having the least or most DON. This confirmed the limited impact of the observed groupings, and we chose to proceed with PLSR using the original data.

QTLs detected by GWAS using MLM

FHB. Based on the GWAS analysis in TASSEL, adjusted for both structure (first three PCA) and kinship (MLM), a QTL on linkage group Mrg12/13A at 41cM for FHB11, FHB12 and FHB_M (Fig. 43) was identified. P-values at this location were statistically significant even using a conservative Bonferroni adjustment for multiple testing (threshold $P \leq 1.95 \times 10^{-5}$). Under the same methods and criterion, associations with FHB11 and FHB_M were also present on linkage groups Mrg02/9D (at 31cM) and Mrg03/4C (at 12cM). However, when FHB was analyzed with DTF as a covariate, none of these QTLs were significant, suggesting that heading date accounted for at least a portion of the FHB effect at these loci. With PH as a covariate, evidence of the association was also reduced at the Mrg03/4C QTL. Conversely, a QTL for FHB11 on

Formatted: Highlight

Mrg20/19A at 21cM was statistically significant only with DTF incorporated as a covariate (not shown in Table 5).

DON. QTLs for DON_11 on Mrg03/4C and DON_12 on Mrg09/6C coincided with FHB QTLs. Evidence of QTLs for DON11were observed on Mrg18/ (3C?) (at 7cM) and also DON_M on Mrg23/11A (at 54cM), but with DON12 only associations were suggested (P<0.0001) at those locations. Both these DON11 QTL were consistent with DTF or PH as covariates.

QTLs detected by GWAS using PLSR

An analysis of individual years and trials showed reasonably similar patterns. For simplicity, only the analysis by mean across years is reported in Table 6, unless otherwise noted.

FHB. Analyses of FHB_M only gave similar results as individual year values (FHB11, FHB12 alone or together). Simultaneous analysis of the three variables FHB_M, DTF_M and DTM_M together is reported to visualize the potential of multivariate QTL analyses in PLSR. The different steps are shown in Figure ~~5A~~4A-F. In Fig. ~~5A~~4A, the blue "cloud" are all the markers, those in circles significant after cross validation. That FHB_M is located in the upper right quadrant and DTM_M (and DTF_M, not seen) in a nearly diagonal position, indicating that later maturity is associated with lower disease scores, confirming the correlations in Table 3. The degrees of explained (calibration) variance along each axis (8%, 34%) refers to explained X (marker) and Y (FHB_M) variance, respectively. The full model indicates calibrated R^2 values of 80.2% of the variation in FHB_M. PC1 is the most important of the five recommended explaining 34,2 % of the validated variance. The score plot (Fig ~~5B~~4B) displayed groupings very similar to those in Fig.~~3~~S1A. The prediction accuracy of the full model is rather poor (Fig. ~~5C~~4C), with the most marked deviations in the most resistant and most susceptible lines.

An optimized model including only significant markers recommended 3 PCs, now explaining 67% of validated variance (box in Fig. ~~5E~~4F), more than twice the model based on all markers. Strikingly, the new score plot (Fig. ~~5E~~4E) displayed two groups not seen in the previous plots (Fig. ~~3~~S1A, Fig. ~~5B~~4B). The smaller contained lines from the Midwest (ILL, PURDUE and WISC) and some from OTTW. The very susceptible Purdue line 'Robust', as well as 'Ogle' and 'Gem', belonged in this group, but some Midwest lines formed the most susceptible part of the

Formatted: Not Highlight
Formatted: Highlight
Formatted: Not Highlight
Formatted: Highlight
Formatted: Not Highlight
Formatted: Highlight
Formatted: Not Highlight
Formatted: Highlight
Formatted: Not Highlight
Formatted: Highlight
Formatted: Not Highlight
Formatted: Highlight
Formatted: Not Highlight
Formatted: Highlight
Formatted: Not Highlight
Formatted: Highlight
Formatted: Not Highlight

other, more variable group. The best and worst checks (represented by the red dot checks in Fig. 5E4E) were much more accurately predicted.

The QTL regions were then analyzed one at a time. On inspecting the linkage group information, relatively few markers discriminated the two groups in Fig. 5E4E, the most significant represented a wide region on Mrg02/9D, spanning from ca 30 to 90 of this 111 cM linkage group. Deleting this region from the analysis removed the groups in Fig. 5E4E. Including *only* this putative QTL in the model led to a marked drop in explained variance and a much poorer prediction (23% calibrated variance, figure not shown), indicating that it was necessary to include several QTLs.

Inspecting the other significant marker regions revealed QTLs on a number of linkage groups (Table 6). Judged from the significance of the regression coefficients after cross-validation, there was evidence for consistent FHB_M QTLs also on Mrg01/?, Mrg03/4C, Mrg04/18D, Mrg11/1C, Mrg12/13A, Mrg13/?, Mrg19/21D and Mrg33/15A.

Including *only* FHB_M in the model showed that except for Mrg03/4C, most FHB_M QTL coincided with QTL for DTF_M and DTM_M. Similarly, repeating the FHB_M analysis with DTF as a covariate reduced the range of values from 2-32% to 7-19% and the predictive ability, except for the most susceptible or resistant.

The co-locations of many QTLs for FHB and phenology is not surprising given the magnitudes of the correlation coefficients (Table 3) and the correlation loadings plot (Fig. 5A4A), where DTF_M and DTM_M were diagonally associated with FHB_M, indicating opposite effects of the alleles at numerous associated, linked or pleiotropic loci. The two suggested PCs explained 34 and 13% of the variance, respectively, but after cross validation only PC1 was significant. The score plot (Fig. 5B4B) displayed a pattern very similar to the PCA in Fig. 3A,S1A. However, the prediction was not good, the validated R^2 being only 34%, against the calibrated 80% (red and blue in Fig. 5C4C). Optimizing models by including only the markers with regression coefficients significant after cross validation markedly improved predictions.

DON. The same procedure for DON_M produced a score plot very similar to that in Fig. 5B 4B and with poor predictions in the lower half of the range (2-15 ppm). In total, 762 markers were identified as significant, explaining 23% of the variance. Optimizing the model improved the R^2 up to 30%, but did not produce two groupings, like in Fig. 5A4E. Many significant markers

Formatted: Highlight
Formatted: Not Highlight
Formatted: Highlight
Formatted: Not Highlight
Formatted: Highlight
Formatted: Not Highlight
Formatted: Highlight
Formatted: Not Highlight
Formatted: Highlight
Formatted: Not Highlight
Formatted: Highlight
Formatted: Not Highlight
Formatted: Highlight
Formatted: Not Highlight
Formatted: Highlight
Formatted: Not Highlight
Formatted: Highlight
Formatted: Not Highlight
Formatted: Highlight
Formatted: Not Highlight
Formatted: Highlight
Formatted: Not Highlight

indicated QTLs common to those found for FHB_M (Table 6), but the ones on Mrg02/9D and Mrg12/13A were less associated with DON_M than FHB_M or DTF.

At least six QTLs associated with DON_M were not affected by DTF (directly or as DON_McovDTF on Mrg01/? (two regions), Mrg04/18D, Mrg05/16A, 1C , Mrg11/1C and Mrg23/11A).That other QTLs were more significant for DON_M than for FHB_M and DTF is consistent with the much lower correlation coefficients in Table 3.

The QTL on Mrg11/1C was only weakly associated with DTF. It was analyzed in greater detail by regressing DON_M, FHB_M and/or DTF on the markers in this linkage group. A group of 28 markers in the 3.3-9.8cM region were polymorphic and clearly associated with DON_M (more in 2011 than 2012) and with FHB_M. In both traits, marker means were significantly different over years. As an example, at the SNP avgbs_62354 allele A (N=186) had a mean value of 16.1 ppm in 2011 and 17.1 in 2012, with a grand mean of 16.6, whereas allele B (N=182) had 12.7, 16.2 and 14.5, respectively (LSD $p<0.01$). For FHB the allelic effects differed by 3.0% in 2011 and 2.3% in 2012, with an A mean of 13.2% and B 10.5%, respectively (LSD $p<0.01$). The difference between the two alleles in DON11 values is easily seen in the score plot in Figure S3, and this locus alone had an R^2 of 10.9% of the variation in DON11 (not shown). Another SNP in this position, the less polymorphic SNP, GMI_GBS_5806 (A=99 and B=327), had similar values. In both, the resistant allele was not associated with any particular germplasm group, so the QTL appeared easily selectable in many breeding programs.

Discussion

Phenotypic evaluation

The present study suggests that lack of genetic variance has previously hindered the assessment of FHB in oat. Weak correlations between FHB and DON (He et al. 2013; Liu et al. 1997; Tekauz et al. 2004) have made FHB symptoms an unreliable predictor of DON. Only with a broader spectrum of susceptibility, as in this study, can significant correlations be expected (Figure 2, Table 2). Nevertheless, correlation coefficients were still not high (r=0.36-0.40), though similar to Rodemann and Niepold (2008) (r=0.38), while in the mapping cross of He et al

Formatted: Not Highlight

(2013) it was -0.19. Due to higher disease pressure, most Nordic and Canadian oats may have accumulated resistance genes, whereas the US oat developed under lower disease pressure had a wider range of responses. The especially susceptible class observed in Fig. ~~5D~~ 4E and Fig. 2 no doubt contributes to the correlation. It is noteworthy that in this study the cv. 'Bessin', used as a highly susceptible check in our trials in Norway (Bjørnstad and Skinnes 2008), had FHB and DON values only slightly higher than the respective grand means. In practical breeding the desirable earliness should be selected before screening for *Fusarium*, and one should pay attention to this during introgression between genepools, else an increased variance may reflect un-adapted germplasm.

The correlations between DTF, DTM or PH with FHB/DON imply that the three possible mechanisms proposed in wheat, i.e. pleiotropy, tight linkage, and disease escape (Buerstmayr et al. 2009; Lu et al. 2013), also apply in oat.

Pleiotropy is probably a real factor in this population. A strong DTF QTL on Mrg02/9D coincides with FHB in TASSEL. Furthermore, the Mrg12/13A DTF QTL, the strongest in Norwegian conditions (Esvelt Klos et al. 2016) , coincides with FHB in TASSEL and FHB and DON in PLSR. We hypothesize that due to photoperiod sensitivity, lines from the Midwest may have a precocious flowering in very long days and possibly immature cell walls, making them very susceptible.

"Escape" due to scoring of FHB at the same dates, rather than according to phenology, easily produces a "pleiotropic" correlation between lateness and resistance(He et al. 2013) . Our use of AUDPC may improve, but not remove such an association, which is more difficult to correct in oat than in wheat. First, the range of DTF within a panicle is wider in oat, on average of 8 days (Misonoo 1936) against 3-6 in wheat (Percival 1921). Second, oat appears more prone to later tillers than wheat or barley. Third, discoloration in glumes occurs early in oat and is easily confounded with Fusarium symptoms. Fourth, some very precocious lines may be associated with softer glume texture that may make florets more susceptible. Fifth, short plants, especially semi-dwarfs like 'Horizon270', are more easily infected in spawn inoculation, since their panicles are closer to the inoculum on the soil surface. Sixth, early lines will have longer exposure to mist irrigation and may remain longer in the field after maturity, especially in case of

Formatted: Highlight

Formatted: Not Highlight

rainy late season. This may of course also lead to differences in temperature during grain filling. Although DON is less affected by scoring time than FHB, humid weather late in grain development may increase DON levels (Tekle et al. 2013).

However, other factors may counteract this. The use of spawn rather than spray inoculation, allowing a continuous presence of ascospores, may better mimic natural conditions (Tekle et al. 2013). Second, the positive correlations between lateness and disease level reported in Finland (Parikka et al. 2008) and Russia (Gavrilova et al. 2008) may be ascribed to rainfall favoring disease in late lines. Third, *Fusarium* kernels infected around anthesis will abort or shrivel before harvest and DON levels underestimated. Our attempt to use sterility-adjusted DON (wDON), under the assumption that all the sterile florets were caused by early infection, was not very successful (Table 2), possibly due to naturally sterile florets frequently observed in un-adapted germplasm susceptible to FHB. In the end only parallel experiments with yield plots without infection is able to assess effects on grain weights and grain yield. Fortunately, the "resistant" entries will be further tested. The FHB check ranking in 2016 corresponds well with the results reported here, with 'Leggett' as the least and 'Bessin' highly infected, though less than the current susceptibility check, the cv. 'Poseidon'. The two years we report are reasonably consistent, but breeding trials with highly selected lines will need more environments. In general, we are confident about the validity of our method in wheat, where our spawn inoculation has correlations about 0.6 with spray inoculations of the same material in CIMMYT (Lillemo, pers. comm.).

Structure and groupings in the population

The lack of clear structure, whether by using model-based methods or PCA or LDA-PCA is consistent with previous studies reporting weak population differentiation in spring oat. The ability of LDA-PCA to identify intuitive and empirically reasonable groupings by breeding programs based on previous knowledge and pedigrees, corroborated the findings by Jombart et al. (2010). However, no groupings mattered much to the later identification of QTL. It would be very interesting to compare LDA-PCA with model-based analyses in more structured plant populations.

Formatted: Not Highlight

QTL detected by GWAS using MLM vs PLSR

Eight of the 10 QTLs for FHB and/or DON detected by TASSEL (Table 5) were also detected by PLSR (Table 6), which also detected 11 others, notably, the QTL on Mrg11/1C. Only Mrg18/(3C?) and Mrg28/(7C-17A?) were unique to TASSEL. In general, PLSR identified more QTLs and those found by TASSEL, possibly due to the adoption of Bonferroni correction in the latter, which may have inflated the false negative rate. However, Bonferroni assumes that tests (variables) are independent, which they are not. Moreover, PLSR is designed to handle the "p>>n" problem, data tables that have many more (and correlated) variables than samples, like in our case. That it also identified the Mrg11/1C QTL reported before (see below), indicates that the method is promising also for GWAS.

However, unlike TASSEL, the *Unscrambler* software used here is not optimized for GWAS, making it rather tedious to run the individual LGs one at a time. As mentioned by Boulesteix and Strimmer (2007), PLSR is available in various formats (like SAS or R) and for many different purposes. The Sparse PLS method does the variable selection and model optimization automatically, possibly with less of the interactive, visually exploratory approach that lends itself to interpreting patterns. A full analysis of PLSR as a method of QTL analysis and GWAS in plants exceeds the scope of this paper, and needs a species more genomically developed than oats. T~~t~~he reader is referred to the paper by Dumancas et al and the aforementioned obesity study (Xue et al. 2012). Especially, we mention the joint analyses of several phenotypic traits and loci at the same time, giving more insight than simple traits or correlations (Fig. ~~5A~~4A-F).

Compared to the GGE analysis (Yan et al. 2005), the cross validation and regression implicit in PLSR allows a straightforward testing and identification of important associations, beyond the visual inspection of biplots or vector lengths and angles. However, it would be very interesting to see PLSR in the GGE framework, due to its ease and breeder/researcher-friendly interface.

Both QTL detection methods used here are "two stage" analyses: first of the phenotypic data, then estimating the allelic effects. "One stage" analysis is preferable(Smith et al. 2001), but are

Formatted: Highlight

Formatted: Not Highlight

Formatted: Not Highlight

Formatted: Not Highlight

Formatted: Not Highlight

Formatted: Not Highlight

Formatted: Not Highlight

Formatted: Not Highlight

Formatted: Not Highlight

computationally heavy, so "two stage" is most usual. Another issue is modelling genotypes as random (BLUPs) or fixed (BLUEs) in the first step. When combining phenotypic data from different experiments, BLUEs are recommended, especially with missing data and unbalanced designs (Piepho et al. 2012), while spatial corrections may make BLUEs correlated. The one stage/two stage issues have been addressed in various ways in human, animal and plant studies, and in a recent simulation study by Holland & co-workers (personal communication and , see http://biorxiv.org/content/early/2017/01/09/099291). They conclude that with balanced data, BLUEs and BLUPs give the same results (like in our data) and as a one-stage method, but if severely unbalanced, BLUEs more often come closer. They have developed a weighting method for BLUEs as part of TASSEL that closely approximates a one-step analysis.

Comparisons with previous mapping studies

The major QTL for FHB detected on Mrg11/1C corresponds in terms of common SNP markers with the major DON QTL *Qdon-umb-17A/7C* detected by He et al. (2013). However, of the 10 SNPs then assigned to 17A/7C, 7 were now mapped on Mrg11/1C, of which five at the 8.8cM position that is homologous to the QTL region in both populations mapped by He et al. (2013), whereas the remaining three were located on the distal region of Mrg05/16A. Therefore, *Qdon-umb-17A/7C* must be located on Mrg11/1C, instead of 17A/7C as reported in He et al. (2013). The average effects of the QTL – from 1-3.5 ppm DON or 2% in FHB -– may seem modest, since both 'Leggett' and 'Horizon270' had the "resistant" allele, but it is independent on DTF and should be easy to select, because the polymorphism was found in most breeding programs.

The major QTL for FHB detected on Mrg12/13A corresponds in terms of common SNP markers with the 13A QTL for DON10, PH and DTF detected by He et al (2013) in the 'Hurdal' x 'Z595-7' population. The close map positions of FHB and DTF, its disappearance when using the latter as a covariate and the phenotypic correlations all confirm that this FHB QTL is closely linked to earliness. Indeed, the strong QTL for DTF in Norway detected in this region by Esvelt Klos et al (2016), indicates a specific photoperiodic response in this long day environment. Notably, few common DON QTLs were detected in our study. The FHB, DTH and DTM QTL on Chr11A of

Formatted: Not Highlight
Formatted: Not Highlight
Formatted: Not Highlight
Formatted: Not Highlight
Formatted: Not Highlight
Formatted: Not Highlight
Formatted: Not Highlight
Field Code Changed
Formatted: Not Highlight
Formatted: Not Highlight
Formatted: Not Highlight
Formatted: Not Highlight
Formatted: Not Highlight
Formatted: Not Highlight
Formatted: Not Highlight
Formatted: Not Highlight
Formatted: Not Highlight
Formatted: Font: Times New Roman, 12 pt, Font color: Text 1
Formatted: Not Highlight
Formatted: Not Highlight
Formatted: Not Highlight
Formatted: Not Highlight
Formatted: Not Highlight
Formatted: Not Highlight
Formatted: Not Highlight

He et al. (2013) corresponded by common markers with ours for DON_M on Mrg23/11A, as did their DON QTL on 5C with our DON_M on Mrg01/5C (although in a quite different position).

Prospects for breeding oats resistant to Fusarium

The consistently low levels of DON and FHB makes 'Leggett' an interesting source of resistance and confirms the results found in Canada (Tekauz et al. 2008; Tekauz et al. 2004). The low DON in the lines having 'Leggett' and 'OT2022' in their pedigree also provide good evidence that DON is a heritable (and unselected) trait. Although not significantly different from the best Nordic line 'Odal', and despite occasional exchanges between the germplasm pools, the sources appear complementary both in markers (Fig ~~3A~~S1A) and pedigrees. The agronomy of 'Leggett' (and most progenies) in Norway was acceptable, approximately 1,5 days later in DTF and 3-6 cm taller, but up to a week later in DTM than Odal, especially in cooler seasons.

Thus, the strong correlations found between phenology (lateness) and *Fusarium* resistance may reflect the germplasm studied, not pleiotropy. Possibly the major QTL for FHB detected on Mrg12/13A represents a photoperiod sensitive adaptation of Midwest oats to mature quickly before temperatures become too high. That the He et al (2013) study was a Norwegian x Midwest cross, may explain why genetic patterns were similar to the current study. The common QTL also increases the relevance of the QTL on Mrg11/1C.Moreover, lateness was more a concern for FHB_M than for DON_M, which is what this study recommends to use, since it is the target trait and appears less associated with phenology. By selecting for DON (supplemented by germination percentage, Tekle et al. 2013) in the disease nursery system used in this study, over less than 10 years Norwegian oat breeding has reduced DON levels by 40-50% in commercial varieties, with approximately similar maturity (Tekle et al 2017, in prep). However, high DON levels – from 1-15 ppm or more - are desirable for screening, and a set of carefully chosen checks to cover this range, are necessary to monitor data from nurseries in different environments to give LSDs less than 3 ppm.

ACKNOWLEDGEMENTS

The authors acknowledge the generous support for this project from:

(1) the Norwegian Research Council Project 199412 (2010-2013) *Mycotoxin contamination in Norw. food and feed - modelling, reductive approaches and risk assessment with regard to the whole food chain* (field and analytical experimental costs)

(2) Graminor AS, responsible for oat breeding in Norway, for support to the mentioned project and the long term collaboration on Fusarium testing;

(3) the Collaborative Oat Research Enterprise by General Mills, the North American Millers Association, the Prairie Oat Growers Association of Canada, USDA-NIFA, and Agriculture and Agri-food Canada,

(4) Eric Jackson, for his vision and leadership of the CORE (multiplication of accessions, production and editing of marker data). We refer the reader to the public T3/Oat database (https://triticeaetoolbox.org/oat) where more data and related meta-data for markers may be downloaded than in the Supplementary File 1,

(5) The first author (ÅB) wishes to thank Dr. Harald Martens for decades of stimulating discussions about multivariate methods in genetics.

Formatted: Not Highlight

Formatted: Not Highlight

References

Asoro FG, Newell MA, Scott MP, Beavis WD, Jannink J-L (2013) Genome-wide Association Study for Beta-glucan Concentration in Elite North American Oat. Crop Science 53:542-553

Bjørnstad Å, Skinnes H (2008) Resistance to *Fusarium* infection in oats (*Avena sativa* L.). Cereal Res Commun 36:57-62

Bjørnstad Å, Westad F, Martens H (2004) Analysis of genetic marker-phenotype relationships by jack-knifed partial least squares regression (PLSR). Hereditas 141:149-165

Boulesteix A-L, Strimmer K (2007) Partial least squares: a versatile tool for the analysis of high-dimensional genomic data. Briefings in Bioinformatics 8:32-44

Bradbury PJ ZZ, Kroon DE, Casstevens TM, Ramdoss Y, Buckler E (2007) TASSEL: Software for association mapping of complex traits in diverse samples. Bioinformatics 23:2633-2635

Buerstmayr H, Ban T, Anderson JA (2009) QTL mapping and marker-assisted selection for *Fusarium* head blight resistance in wheat: a review. Plant breeding 128:1-26

Campbell H, Choo TM, Vigier B, Underhill L (2000) Mycotoxins in barley and oat samples from eastern Canada. Canadian Journal of Plant Science 80:977-980

Chaffin AS, Huang Y-F, Smith S, Bekele WA, Babiker E, Gnanesh BN, Foresman BJ, Blanchard SG, Jay JJ, Reid RW, Wight CP, Chao S, Oliver R, Islamovic E, Kolb FL, McCartney C, Mitchell Fetch JW, Beattie AD, Bjørnstad Å, Bonman JM, Langdon T, Howarth CJ, Brouwer CR, Jellen EN, Klos KE, Poland JA, Hsieh T-F, Brown R, Jackson E, Schlueter JA, Tinker NA (2016) A Consensus Map in Cultivated Hexaploid Oat Reveals Conserved Grass Synteny with Substantial Subgenome Rearrangement. The Plant Genome 9

Dumancas GG, Ramasahayam S, Bello G, Hughes J, Kramer R (2015) Chemometric regression techniques as emerging, powerful tools in genetic association studies. TrAC Trends in Analytical Chemistry 74:79-88

Emrich K, Wilde F, Miedaner T, Piepho HP (2008) REML approach for adjusting the *Fusarium* head blight rating to a phenological date in inoculated selection experiments of wheat. Theoretical and applied genetics 117:65-73

Esvelt Klos K, Huang Y-F, Babiker E, Beattie A, Bjørnstad A, Bonman M, Carson M, Chao S, Gnanesh B, Grifiths I, Harrison S, Howarth C, Hu G, Ibrahim A, Islamovic E, Jackson E, Jannink J, Kolb F, McMullen M, Mitchell Fetch J, Murphy J, Ohm H, Rines H, Rossnagel B, Schlueter J, Sorrells M, Wight C, Yan W, Tinker N (2016) Population genomics related to adaptation in elite oat germplasm. . The Plant Genome

European Commission (2006) Commission Regulation (EC) No. 1881/2006 setting maximum levels of certain contaminants in foodstuffs. Off J Eur Union L364:5–24

Fuentes RG, Mickelson HR, Busch RH, Dill-Macky R, Evans CK, Thompson WG, Wiersma JV, Xie W, Dong Y, Anderson JA (2005) Resource allocation and cultivar stability in breeding for Fusarium head blight resistance in spring wheat. Crop Science 45:1965-1972

Gavrilova O, Gagkaeva T, Burkin A, Kononenko G, Loskutov I (2008) Susceptibility of oat germplasm to *Fusarium* infection and mycotoxin accumulation in grains. Proceedings of the 8th International Oat Conference, Minneapolis, MN, USA, pp 7–16

He X, Skinnes H, Oliver RE, Jackson EW, Bjørnstad Å (2013) Linkage mapping and identification of QTL affecting deoxynivalenol (DON) content (Fusarium resistance) in oats (Avena sativa L.). Theoretical and applied genetics 126:2655-2670

Huang Y-F, Poland JA, Wight CP, Jackson EW, Tinker NA (2014) Using Genotyping-By-Sequencing (GBS) for Genomic Discovery in Cultivated Oat. PLoS ONE 9:e102448

Jombart T, Devillard S, Balloux F (2010) Discriminant analysis of principal components: a new method for the analysis of genetically structured populations. BMC Genetics 11:94

Kollers S, Rodemann B, Ling J, Korzun V, Ebmeyer E, Argillier O, Hinze M, Plieske J, Kulosa D, Ganal MW, Roder MS (2013) Whole genome association mapping of Fusarium head blight resistance in European winter wheat (Triticum aestivum L.). PLoS One 8:e57500

Langevin F, Eudes F, Comeau A (2004) Effect of trichothecenes produced by *Fusarium graminearum* during Fusarium head blight development in six cereal species. European Journal of Plant Pathology 110:735-746

Langseth W, Hoie R, Gullord M (1995) The Influence of Cultivars, Location and Climate on Deoxynivalenol Contamination in Norwegian Oats 1985-1990. Acta Agr Scand B-S P 45:63-67

Liu WZ, Langseth W, Skinnes H, Elen ON, Sundheim L (1997) Comparison of visual head blight ratings, seed infection levels, and deoxynivalenol production for assessment of resistance in cereals inoculated with *Fusarium culmorum*. European Journal of Plant Pathology 103:589-595

Lu Q, Lillemo M, Skinnes H, He X, Shi J, Ji F, Dong Y, Bjornstad A (2013) Anther extrusion and plant height are associated with Type I resistance to Fusarium head blight in bread wheat line 'Shanghai-3/Catbird'. Theoretical and Applied Genetics 126:317-334

Marshall A, Cowan S, Edwards S, Griffiths I, Howarth C, Langdon T, White E (2013) Crops that feed the world 9. Oats- a cereal crop for human and livestock feed with industrial applications. Food Sec 5:13-33

Martens H, Kohler A (2009) Mathematics and measurements for high-throughput quantitative biology. Biological Theory 4:29-43

Martens H, Naes T (1992) Multivariate calibration. John Wiley & Sons

Massman J, Cooper B, Horsley R, Neate S, Dill-Macky R, Chao S, Dong Y, Schwarz P, Muehlbauer GJ, Smith KP (2011) Genome-wide association mapping of Fusarium head blight resistance in contemporary barley breeding germplasm. Molecular Breeding 27:439-454

Mirocha CJ, Kolaczkowski E, Xie WP, Yu H, Jelen H (1998) Analysis of deoxynivalenol and its derivatives (batch and single kernel) using gas chromatography mass spectrometry. J Agr Food Chem 46:1414-1418

Misonoo G (1936) Ecological and physiological studies on the blooming of oat flowers. Journal of the Faculty of Agriculture, Hokkaido Imperial University= 北海道帝國大學農學部紀要 37:211-337

Nei M (1973) Analysis of Gene Diversity in Subdivided Populations. Proc Natl Acad Sci U S A 70:3321-3323

Newell M, Cook D, Tinker N, Jannink JL (2010) Population structure and linkage disequilibrium in oat (*Avena sativa* L.): implications for genome-wide association studies. Theoretical and Applied Genetics:1-10

Newell MA, Asoro FG, Scott MP, White PJ, Beavis WD, Jannink JL (2012) Genome-wide association study for oat (Avena sativa L.) beta-glucan concentration using germplasm of worldwide origin. Theoretical and Applied Genetics 125:1687-1696

Oliver RE, Lazo GR, Lutz JD, Rubenfield MJ, Tinker NA, Anderson JM, Wisniewski Morehead NH, Adhikary D, Jellen EN, Maughan PJ, Brown Guedira GL, Chao S, Beattie AD, Carson ML, Rines HW, Obert DE, Bonman JM, Jackson EW (2011) Model SNP development for complex genomes based on hexaploid oat using high-throughput 454 sequencing technology. BMC Genomics 12:77

Oliver RE, Obert DE, Hu G, Bonman JM, O'Leary-Jepsen E, Jackson EW (2010) Development of oat-based markers from barley and wheat microsatellites. Genome 53:458-471

Oliver RE, Tinker NA, Lazo GR, Chao S, Jellen EN, Carson ML, Rines HW, Obert DE, Lutz JD, Shackelford I, Korol AB, Wight CP, Gardner KM, Hattori J, Beattie AD, Bjornstad A, Bonman JM, Jannink JL, Sorrells ME, Brown-Guedira GL, Mitchell Fetch JW, Harrison SA, Howarth CJ, Ibrahim A, Kolb FL, McMullen MS, Murphy JP, Ohm HW, Rossnagel BG, Yan W, Miclaus KJ, Hiller J, Maughan PJ, Redman Hulse RR, Anderson JM, Islamovic E, Jackson EW (2013) SNP discovery and chromosome anchoring provide the first physically-anchored hexaploid oat map and reveal synteny with model species. PLoS One 8:e58068

Parikka P, Hietaniemi V, Rämö S, Jalli H (2008) Fusarium infection and mycotoxin contents of oats under different tillage treatments. Proceedings of the 8th International Oat Conference, Minneapolis, MN, USA

Peakall R, Smouse PE (2006) GENALEX 6: genetic analysis in Excel. Population genetic software for teaching and research. Mol Ecol Notes 6:288-295

Percival J (1921) The Wheat Plant. Duckworth & Co, London

Piepho HP, Möhring J, Schulz-Streeck T, Ogutu JO (2012) A stage-wise approach for the analysis of multi-environment trials. Biometrical Journal 54:844-860

Price AL, Zaitlen NA, Reich D, Patterson N (2010) New approaches to population stratification in genome-wide association studies. Nat Rev Genet 11:459-463

Pritchard JK, Stephens M, Donnelly P (2000) Inference of Population Structure Using Multilocus Genotype Data. Genetics 155:945-959

Rines H, Molnar S, Tinker N, Phillips R (2006) Oat. In: Kole C (ed) Genome Mapping and Molecular Breeding in Plants, Cereals and Millets. Springer-Verlag, Berlin, pp 211-242

Rodemann B, Niepold F (2008) Susceptibility of oat varieties against Fusarium head blight. Cereal Research Communications 36:719-721

Scott RA, Milliken GA (1993) A SAS program for analyzing augmented randomized complete-block designs. Crop Science 33:865-867

Skinnes H, Semagn K, Tarkegne Y, Marøy AG, Bjørnstad Å (2010) The inheritance of anther extrusion in hexaploid wheat and its relationship to *Fusarium* head blight resistance and deoxynivalenol content. Plant breeding 129:149-155

Smith A, Cullis B, Gilmour A (2001) Applications: the analysis of crop variety evaluation data in Australia. Australian & New Zealand Journal of Statistics 43:129-145

Steffenson B, Leonard K, Bushnell W (2003) Fusarium head blight of barley: impact, epidemics, management, and strategies for identifying and utilizing genetic resistance. In: Leonard K, Bushnell W (eds) Fusarium head blight of wheat and barley, pp 241-295

Tekauz A, Fetch JM, Rossnagel B, Savard M (2008) Progress in assessing the impact of Fusarium head blight on oat in western Canada and screening of avena germplasm for resistance. Cereal Research Communications 36:49-56

Tekauz A, McCallum B, Ames N, Fetch JM (2004) Fusarium head blight of oat — current status in western Canada. Canadian Journal of Plant Pathology 26:473-479

Tekle S, Dill-Macky R, Skinnes H, Tronsmo AM, Bjornstad A (2012) Infection process of *Fusarium graminearum* in oats (*Avena sativa* L.). European Journal of Plant Pathology 132:431-442

Tekle S, Skinnes H, Bjornstad A (2013) The germination problem of oat seed lots affected by Fusarium head blight. European Journal of Plant Pathology 135:147-158

Tinker NA, Chao S, Lazo GR, Oliver RE, Huang Y-F, Poland JA, Jellen EN, Maughan PJ, Kilian A, Jackson EW (2014) A SNP Genotyping Array for Hexaploid Oat. The Plant Genome 7

Tinker NA, Kilian A, Wight CP, Heller-Uszynska K, Wenzl P, Rines HW, Bjornstad A, Howarth CJ, Jannink JL, Anderson JM, Rossnagel BG, Stuthman DD, Sorrells ME, Jackson EW, Tuvesson S, Kolb FL, Olsson O, Federizzi LC, Carson ML, Ohm HW, Molnar SJ, Scoles GJ, Eckstein PE, Bonman JM, Ceplitis A, Langdon T (2009) New DArT markers for oat provide enhanced map coverage and global germplasm characterization. BMC Genomics 10:39

Xue F, Li S, Luan Ja, Yuan Z, Luben RN, Khaw K-T, Wareham NJ, Loos RJF, Zhao JH (2012) A Latent Variable Partial Least Squares Path Modeling Approach to Regional Association and Polygenic Effect with Applications to a Human Obesity Study. PLoS ONE 7:e31927

Yan W, Tinker NA (2005) A biplot approach for investigating QTL-by-environment patterns. Molecular Breeding 15:31-43

Yan W, Tinker NA, Falk DE (2005) QTL identification, mega-environment classification, and strategy development for marker-based selection using biplots. Journal of Crop Improvement 14:299-324

Zadoks JC, Chang TT, Kozak CF (1974) A decimal code for the growth stages of cereals. Weed Research 14:415-421

Zhu C, Gore M, Buckler ES, Yu J (2008) Status and prospects of association mapping in plants. The Plant Genome

Table 1. Analysis of variance for Fusarium head blight, DON content, and FS in the CORE population

Traits	Source	DF	Mean square	*F* value	*P* value
FHB	Genotype(Check)	421	90.11	5.66	<0.0001
	Check	6	1149.35	72.20	<0.0001
	Year	1	65.31	4.10	0.0435
	Block(Year)	14	12.89	0.81	0.6589
	Column(Year)	78	25.50	1.60	0.0020
	Check*Year	6	105.99	6.66	<0.0001
	Error	403	15.92		
DON	Genotype(Check)	423	95.75	2.10	<0.0001
	Check	6	374.39	8.20	<0.0001
	Year	1	91.77	2.01	0.1570
	Block(Year)	14	62.35	1.37	0.1664
	Column(Year)	78	91.46	2.00	<0.0001
	Check*Year	6	22.36	0.49	0.8160
	Error	405	45.64		
FS	Genotype	414	51.36	5.19	0.0348
	Check	6	103.58	10.46	0.0104
	Block	7	11.08	1.12	0.4667
	Column	30	20.10	2.03	0.2208
	Error	5	9.90		

Table 2. Pearson correlation coefficients among FHB and DON traits in the CORE population

	FHB11	FHB12	FHB_M	DON11	DON12	wDON12	DON_M
FHB11	1						
FHB12	0.70***	1					
FHB_M	0.93***	0.91***	1				
DON11	0.37***	0.33***	0.38***	1			
DON12	0.26***	0.39***	0.34***	0.38***	1		
wDON12	0.28***	0.40***	0.36***	0.39***	0.95***	1	
DON_M	0.39***	0.41***	0.43***	0.88***	0.77***	0.74***	1

*** $P<0.0001$

Table 3. Pearson correlation coefficients between FHB traits and agronomic traits in the CORE population

	DTF	DTM	PH	FS
FHB11	-0.75***	-0.48***	-0.50***	0.19***
FHB12	-0.73***	-0.57***	-0.43***	0.24***
FHB_M	-0.81***	-0.62***	-0.52***	0.23***
DON11	-0.22***	-0.07	-0.21***	0.22***
DON12	-0.25***	-0.13*	-0.21***	0.27***
wDON12	-0.26***	-0.16*	-0.19***	0.49***
DON_M	-0.28***	-0.14*	-0.24***	0.28***

* $P<0.01$, ** $P<0.001$, *** $P<0.0001$

Table 4. A. Results from linear discriminant analysis of the 11 breeding programs based on 1932 SNP markers. This "confusion matrix" shows the correct groupings in the column headers, the predicted grouping in the rows. Correct classifications are along the diagonal. (Distance parameter is Quadratic)

Actual Predicted	PURD	ABER	WNPG	OTTW	NORD	NRWY	SASK	ILL	NDSU	MINN	WISC
PURD	26	0	0	3	0	0	0	3	1	2	0
ABER	0	43	0	1	0	0	0	0	0	0	0
WNPG	0	0	36	3	0	0	8	0	4	5	0
OTTW	0	1	0	16	0	0	8	3	1	1	0
NORD	0	0	0	1	11	2	0	0	0	0	0
NRWY	1	0	0	0	0	13	1	0	0	0	0
SASK	0	1	1	9	0	0	20	0	0	1	0
ILL	1	0	0	0	0	0	1	25	0	4	5
NDSU	1	0	2	4	0	0	2	0	38	3	3
MINN	3	1	1	6	0	0	3	6	4	17	5
WISC	2	0	0	2	0	0	1	9	0	6	34

B. Results from linear discriminant analysis of the four merged "germplasm groups".

Actual Predicted	MIDWEST	ABER	CAN+ND	NORDIC
MIDWEST	141	1	22	0
ABER	1	44	1	0
CAN+ND	23	1	153	0
NORDIC	1	0	1	26

Table 5. QTL influencing FHB and DON as detected by TASSEL. For definition of linkage groups (LG) and tentative assignments to chromosomes (Fletcher et al. (2015) submitted, if in parentheses as in Oliver et al. 2013)

LG	Location (cM)	Trait	Marker	p	neglog10(p)
Mrg01/?	109	FHB11	avgbs_121575	6.50E-05	4.187171841
Mrg02/9D	31	FHB12	GMI_DS_LB_6375	4.68E-05	4.330083792
Mrg02/9D	31	FHB_M	GMI_DS_LB_6375	0.000108	3.965369046
Mrg03/4C	12	FHB_M	avgbs_65698	9.58E-06	5.018744173
Mrg03/4C	12	FHB11	avgbs_65698	1.85E-05	4.732029454
Mrg03/4C	28	DON11	GMI_ES17_c3969_600	8.31E-05	4.080295319
Mrg03/4C	124	FHB11	avgbs_111522	4.88E-05	4.311272263
Mrg09/6C	47	DON_M	avgbs_66173	4.61E-05	4.336509005
Mrg09/6C	47	DON12	avgbs_66173	7.74E-05	4.11147407
Mrg12/13A	41	FHB_M	avgbs_109651	2.61E-06	5.583870058
Mrg12/13A	41	FHB_M	GMI_DS_LB_5810	5.49E-06	5.260173779
Mrg12/13A	41	FHB11	avgbs_109651	8.33E-06	5.079240873
Mrg12/13A	41	FHB11	GMI_DS_LB_5810	4.73E-05	4.324835565

Mrg12/13A	41	FHB_M	GMI_ES03_c14909_90	1.20E-09	8.919983608
Mrg12/13A	41	FHB12	GMI_ES03_c14909_90	1.56E-07	6.806740179
Mrg12/13A	41	FHB11	GMI_ES03_c14909_90	1.06E-06	5.975298543
Mrg18/(3C?)	7	DON11	avgbs_239148	8.64E-06	5.063248071
Mrg23/11A	54	DON11	avgbs_200288	3.18E-07	6.497042714
Mrg23/11A	54	DON_M	avgbs_200288	8.72E-05	4.059327648
Mrg28(7C-17A?)	58	DON12	avgbs_6K_4542	9.75E-05	4.010921594

Table 6. QTLs influencing FHB and DON as detected by PLSR. X = detected, else open. Linkage groups as in DTF= Days to Flowering, FHB or DON_COVDTF are values with DTF as a covariate. The Coincidence column compares with Table 5. Yellow colour signifies QTLs affecting FHB, DON and DTF, amber only DON.

Loci spanning approximate region	Chr	cM	FHB_M	FHB_COVDTF	DON_M	DON_MCOVDTF	DTF	Coincidence with QTL in TASSEL
avgbs_16044-avgbs_33904	Mrg01/?	6,1-12,9	x	x	x	x	x	Not in TASSEL
GMI_ES17_lrc20172_521-GMI_ES03_c447_586	Mrg01/?	34-39			x	x		Not in TASSEL
GMI_ES15_c6458_250-GMI_ES03_c3525_308	Mrg01/?	70,3-89,6	x	x	-	-	x	Not in TASSEL
GMI_GBS_55191-GMI_ES_CC13076_70	Mrg01/?	105,7-112,8	-	-	x	x		The same as the FHB_M QTL at avgbs_121575 in TASSEL
GMI_ES02_c2274_247-GMI_ES17_c7387_367	Mrg02/9D	70,6-87,3	x	x	x	x	x	Significant deviation from TASSEL, but inconsistent marker orders and close to a wide gap
avgbs_222981-avgbs_213850	Mrg03/4C	27,6-37,7	x			x		Most likely the same as the FHB_M QTL at avgbs_65698 at 12 cM and DON_M at GMI_ES17_c3969_600
avgbs_202886-GMI_ES14_c1051_767	Mrg03/4C	80,1-83,8		x	x	x		Not in TASSEL
GMI_ES02_c24274_326-GMI_ES22_c8650_112	Mrg03/4C	118,4-128,6	x	x		x		The same as the FHB11 QTL at avgbs_111522 in TASSEL
avgbs_214940-GMI_ES05_c11381_538	Mrg04/18D	7,1-29,7	x	x	x	x	x	Not in TASSEL
GMI_GBS_13021-GMI_ES_CC9782_260	Mrg04/18D	44,7.45,6			x	x		Not in TASSEL
GMI_GBS_106778-GMI_ES02_c37239_433	Mrg05/16A	28,3-42,2		(x)	x	x		Not in TASSEL

GMI_ES_LB_8449-avgbs_115262	Mrg05/16A	92,1-114,7		(x)	x	x		Not in TASSEL
GMI_ES02_c28827_474-GMI_GBS_6566	Mrg09/6C	32,4-44,7	x	x	x	x	x	The same as the DON_M and DON_11 QTL s at avgbs_66173 in TASSEL
GMI_ES11_c2261_56-GMI_GBS_5806	Mrg11/1C	3,7-8,8	x	x	x	x	(x)	Not in TASSEL
GMI_DS_LB_302-avgbs_95344	Mrg12/13A	17-44,5	x	x		x	x	The same as the FHB and DTF QTLs at position 41 in TASSEL
avgbs_71868-GMI_ES14_c4050_361	Mrg13/?	65,6-68,7	x	(x)	(x)	x	x	Not in TASSEL
avgbs_6K_70597-GMI_GBS_70597	Mrg19/21D	52,1-52,8	x	x	x	x	x	Not in TASSEL
avgbs_213293-GMI_ES17_c244_1098	Mrg23/11A	55,2-59,1			x	x		The same as the DON_M QTL at avgbs_200288 in TASSEL
GMI_ES03_lrc22616_280-GMI_ES05_c16490_161	Mrg33/15A_p	41,4-58,2	x		x	x	x	Not in TASSEL

Legends to the figures

Figure 1. Distribution of the BLUP values for FHB and DON in 2011 and 2012.

Figure 2 Scatter plots for DON vs. FHB using BLUP data. The far right check is 'Horizon270' and the far left is 'Leggett'.

Figure 3. Manhattan plots of –log10(p-values) from mixed linear model (MLM) tests of association for FHB_M (upper) and DON_M (lower) in the CORE population. Note differences in scales of Y-axes.

Figure 4. Steps in the PLSR analyses of FHB_M, DTF_M and DM_M regressed on marker variables.

A. *Correlation loadings bi-plot*, where the axes are scaled as correlation coefficients between -1 and +1. FHB_M, DF_M and DM_M are regressed on *all* markers to identify significant associations. Markers in circles are significant, in the sense that their regression coefficient (from the XXX-dimensional PLSR model) are clearly different from zero for one or more of the regressands FHB_M, DF_M and DM_M, based on their 95% confidence intervals estimated by jack-knifing: leave-one-genotype-out cross validation. (The inner circle transects the axes at ca 0.7, meaning that for markers (blue points) that fall outside it, the model explains >ca. 50% of the variance (R^2>0.7 x 0.7). For the markers closest to FHB_M the highest scores (allele 1) of the SNPs are associated with the highest disease scores and are most susceptible, or vice versa in diagonal positions. In green may be discerned the diagonally opposite positions of DM_M and DT_M, which displays their negative correlations with FHB. The degrees of explained *calibrated* variance along each axis (8%, 34%) refers to explained X (marker) and Y (FHB_M) variance, respectively. The model indicates R^2 values of 34% (Factor-1) and 13% (Factor-2) of the variation in FHB_M. Some markers along axis 2 (bottom of plot) seem only associated with this PC.
B. The corresponding *score plot*, genotypes (samples) color coded according to breeding program, those to the right are closest to FHB_M and most

susceptible. The check (red dot) to the right is the susceptible check 'Horizon270', the check to the left is Leggett.

C. The corresponding regression line showing fit of prediction. *Blue* values correspond to the calibration model including all markers(the full model), *red* the result after cross validation, also using the full model. Note the markedly lower R^2 and the high discrepancy in prediction of the check 'Horizon270' (right). This indicates a typically suboptimal model with uninformative markers. The model identifies 5 PCs, but this may be unnecessarily many. The non-significant markers are not associated with the traits and should not be included in the model.

D. Second round *correlation loadings bi-plot*, including only markers significant identified above. Note that more markers are now located outside the inner ellipse and positively associated with FHB_M or phenology (in green). Note the marked increase in R^2-values, but this is again an overestimation. The cross-validated values are a bit lower, 42.1% and 18.3%, but now with only three recommended PCs.

E. The new *score plot* shows a somewhat changed pattern, since the PLSR *weighs* the loadings in X with regard to Y. The range from susceptible (right) to resistant remains, but with a tendency towards two groups, the one to the right more susceptible and that the Midwest and OTTW have members in each group. ABER is different as before (along PC3). The checks (red dots) 'Horizon270' and 'Leggett' represent two groups.

F. The new prediction plot shows a major improvement in fit (67% of the validated variance) due to the model optimization. Note the better fit for 'Horizon270'.

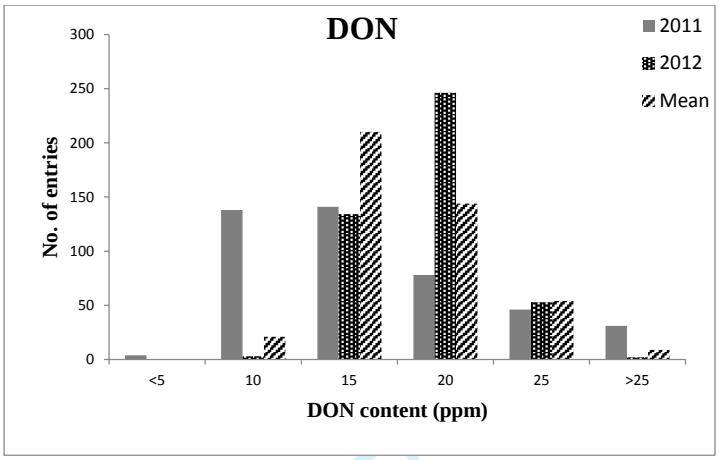
DON
2011
2012
Mean
No. of entries
300
250
200
150
100
50
0
<5
10
15
20
25
>25
DON content (ppm)

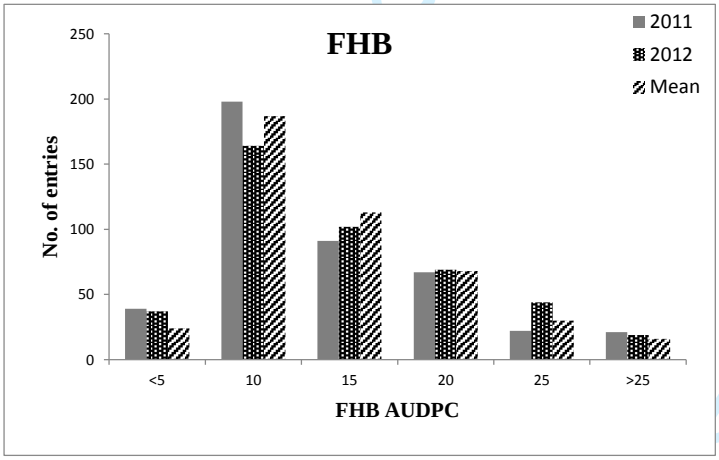
FHB
2011
2012
Mean
No. of entries
250
200
150
100
50
0
<5
10
15
20
25
>25
FHB AUDPC

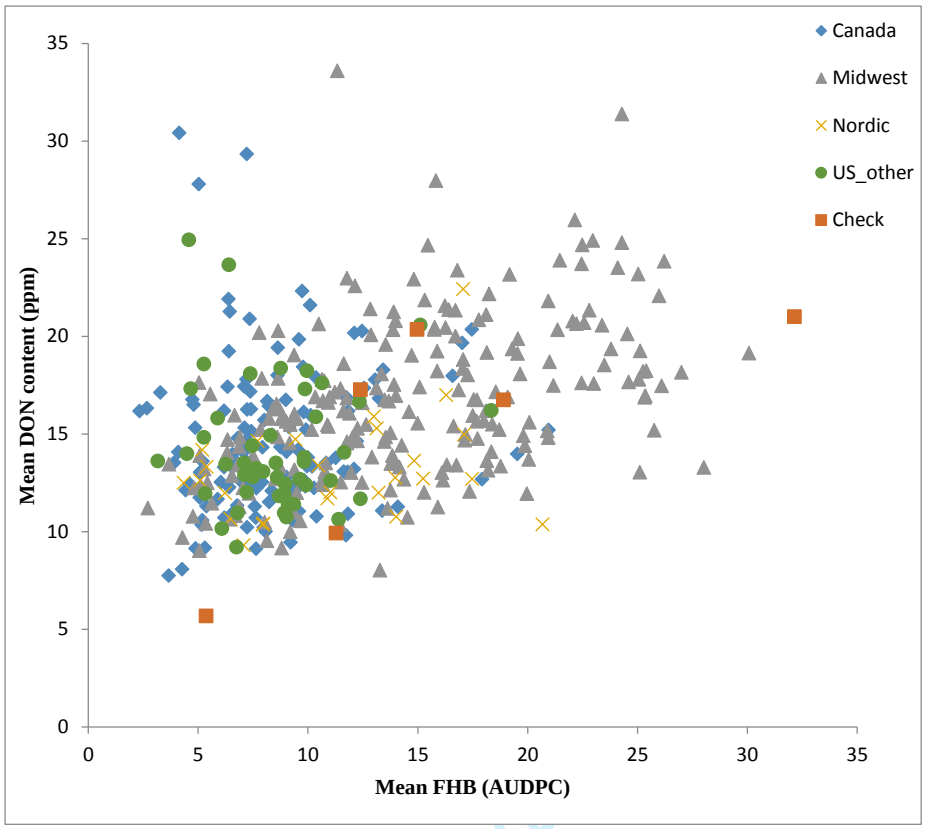


FHB_M
-Log10(p-value)
position
Linkage Group
Mrg01
Mrg02
Mrg03
Mrg04
Mrg05
Mrg06
Mrg08
Mrg09
Mrg11
Mrg12
Mrg13
Mrg15
Mrg17
Mrg18
Mrg19
Mrg20
Mrg21
Mrg23
Mrg24
Mrg28
Mrg33
DON_M
-Log10(p-value)
position
Linkage Group
Mrg01
Mrg02
Mrg03
Mrg04
Mrg05
Mrg06
Mrg08
Mrg09
Mrg11
Mrg12
Mrg13
Mrg15
Mrg17
Mrg18
Mrg19
Mrg20
Mrg21
Mrg23
Mrg24
Mrg28
Mrg33

Figure 4A

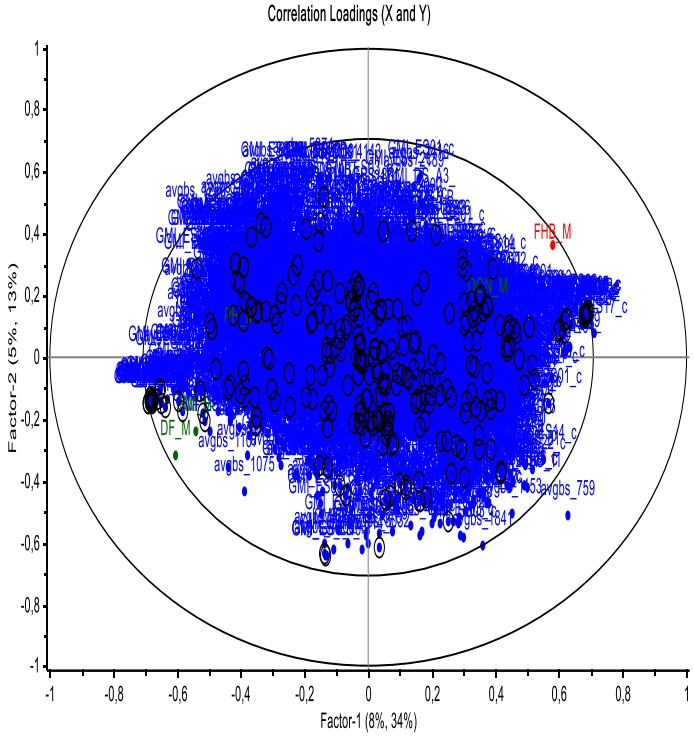
Correlation Loadings (X and Y)
Factor-2 (5%, 13%)
Factor-1 (8%, 34%)
FHB_M
DF_M
1
0,8
0,6
0,4
0,2
0
-0,2
-0,4
-0,6
-0,8
-1
-1
-0,8
-0,6
-0,4
-0,2
0
0,2
0,4
0,6
0,8
1

Fig. 4B.

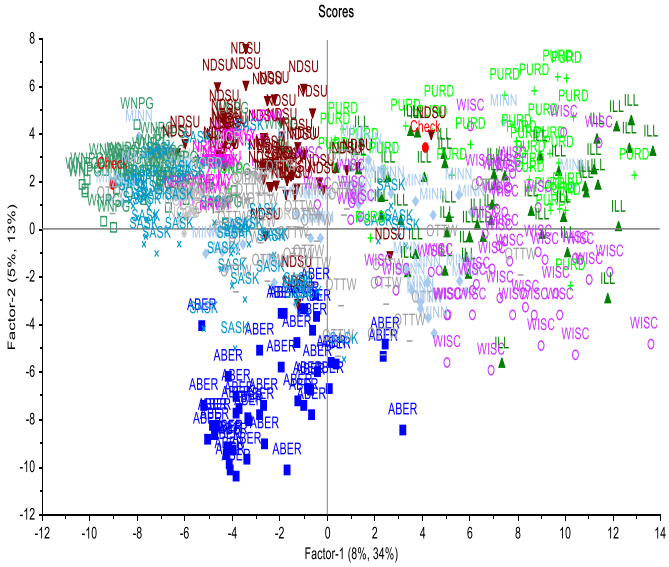

Fig. 4C

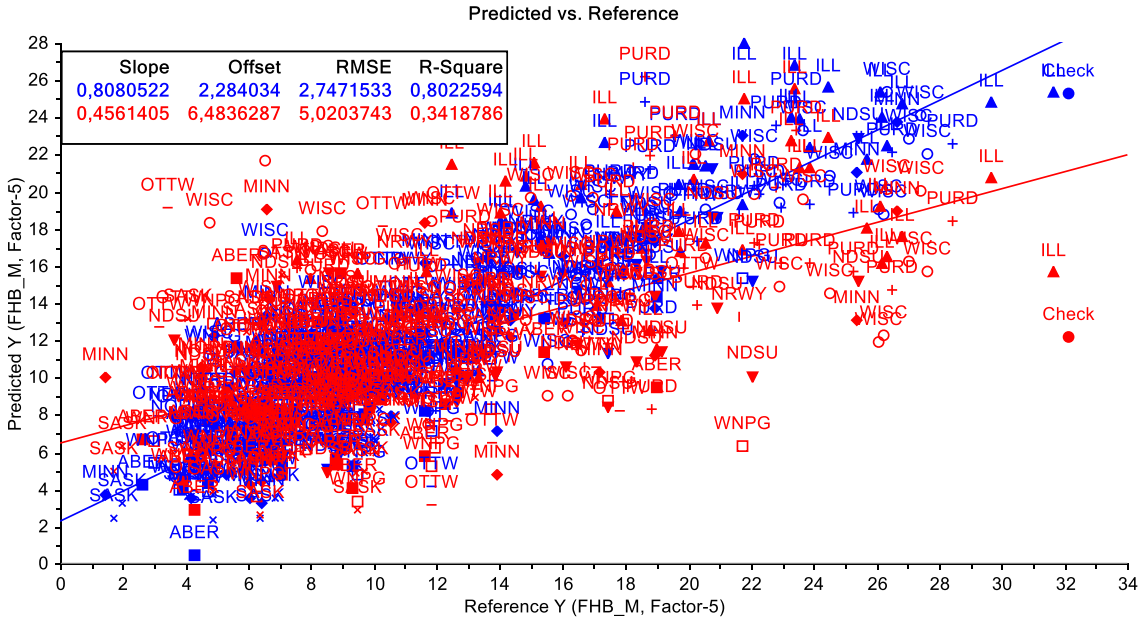

Fig. 4D

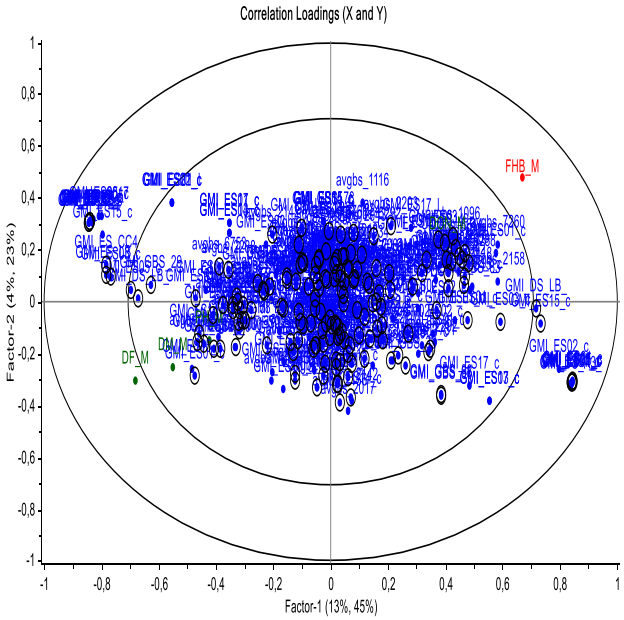

Fig 4E

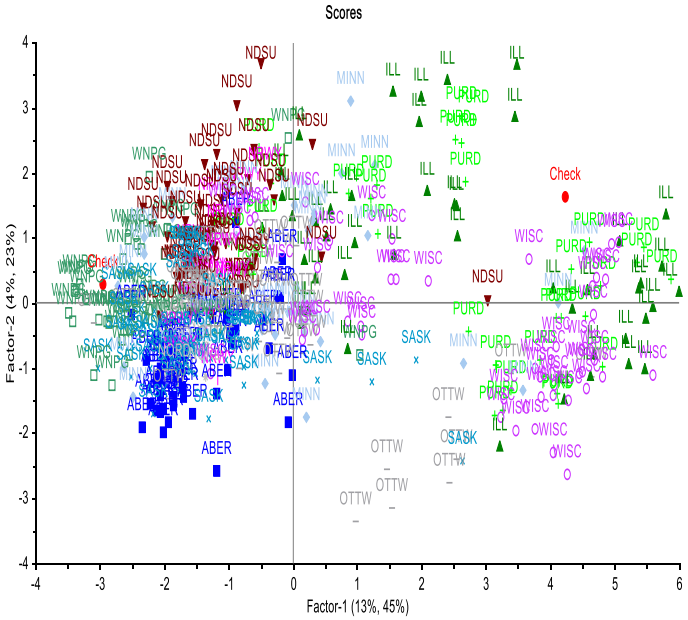

Fig 4F